

Adsorption of acetic and trifluoroacetic acid on the $\text{TiO}_2(110)$ surface

A. S. Foster^{a)} and R. M. Nieminen

Laboratory of Physics, Helsinki University of Technology, P.O. Box 1100, Helsinki 02015, Finland

(Received 8 June 2004; accepted 11 August 2004)

We use the first-principles static and dynamic simulations to study the adsorption of acetic (CH_3COOH) and trifluoroacetic (CF_3COOH) acid on the $\text{TiO}_2(110)$ surface. The most favorable adsorption for both molecules is a dissociative process, which results in the two oxygens of the carboxylate ion bonding to in-plane titanium atoms in the surface. The remaining proton then bonds to a bridging oxygen site, forming a hydroxyl group. We further show that, by comparing the calculated dipoles of the molecules on the surface, it is possible to understand the difference in contrast over the acetate and trifluoroacetate molecules in the atomically resolved noncontact atomic force microscopy images. © 2004 American Institute of Physics. [DOI: 10.1063/1.1802652]

I. INTRODUCTION

The importance of the titanium dioxide (TiO_2) surface in a wide variety of applications, from photocatalysis to bio-medical implants,^{1–4} has led to a considerable research effort to understand its properties. The basic physical and electronic structure of the most stable (110) surface has been well studied both experimentally^{5,6} and theoretically,^{7–11} and now, many investigations focus on defected surfaces, especially oxygen vacancies,^{12–14} adsorption,^{10,15–17} or even adsorption onto defected surfaces.^{18–20} Due to their particular relevance to catalysis, many studies have also investigated the properties of adsorbed carboxylic (RCOOH) acids on the $\text{TiO}_2(110)$ surface. The simplest member of this acid group, formate (HCOOH), has been studied extensively^{21–25} and undergone a dissociative reaction upon adsorption into a carboxylate ion and a proton ($\text{RCOOH} \Rightarrow \text{RCOO}^- + \text{H}^+$). Some experimental studies on acetate (CH_3COOH) adsorption^{26,27} have also been performed providing some basic properties, but a similar level of understanding to formate adsorption is lacking.

Noncontact atomic force microscopy (NC-AFM)^{28,29} studies of formate adsorption on TiO_2 Ref. 23 provided one of the first nontrivial interpretations of atomically resolved images. By combining NC-AFM with scanning tunneling microscopy, they were able to identify the source of contrast in images of the clean surface. This prompted an extensive NC-AFM study^{30–35} of both the acetate and trifluoroacetate (CF_3COOH , referred to as 3F-acetate) adsorption on the surface. This remains the only fully systematic study of adsorption in atomically resolved NC-AFM and is also an important general study of imaging organic layers with this emerging technique. As such, it is crucial that the mechanism of imaging is understood in detail.

In this work, we use first-principles calculations to study the mechanisms of the acetate and 3F-acetate adsorption on the $\text{TiO}_2(110)$ surface and consider the implications for understanding the results of the NC-AFM experiments. Throughout the text, we will refer, in general, to the common

properties of acetate and 3F-acetate and only differentiate them when necessary. We will also use the general formula CX_3COOH .

II. METHODS

All the calculations were performed using the linear combination of atomic orbitals basis SIESTA code,^{36,37} which implements the density functional theory in a manner so as to achieve linear scaling in the construction of the Hamiltonian and overlap matrices. Solution of the self-consistent problem can also be performed with linear scaling for insulators, though here, a full diagonalization is employed so that the electronic structure of the surfaces can be studied in detail. The generalized gradient approximation has been utilized in all the calculations, based on the specific functional of Perdew, Burke, and Ernzerhof.³⁸ Core electrons are represented by norm-conserving pseudopotentials of the form proposed by Troullier-Martins,³⁷ and we use the partial core correction scheme of Louie *et al.*³⁹ All the calculations were spin polarized and implemented a Dirac scalar relativistic correction. The pseudopotential for the titanium atom was generated in the electron configuration $[\text{Ar}]4s^23d^2$, oxygen in $[1s^2]2s^22p^4$, hydrogen in $1s^1$, carbon in $[1s^2]2s^22p^2$, and that for fluorine in $[1s^2]2s^22p^5$, where the square brackets denote the core electron configurations. Various basis set configurations were tested, and a good compromise between accuracy and efficiency was found using a double zeta with polarization for Ti, H, C, and F, and using a triple zeta with polarization for O. All relevant properties of the systems calculated were converged with respect to k -points, mesh cutoff, and orbital cutoffs (i.e., energy shift³⁷).

III. ISOLATED MOLECULES AND SURFACE

As a check for the method and to see how the properties change during adsorption, initial calculations were made on the isolated molecules. The calculated and experimental properties of the two molecules are given in Table I and shown in Fig. 1(a), and generally, the agreement is excellent. Only for the 3F-acetate molecule do we see any significant

^{a)}Electronic mail: asf@fyslab.hut.fi

TABLE I. Comparison of the molecular properties calculated in this work and experiment (Ref. 40). Bond lengths are in angstroms, bond angles are in degrees, and dipoles are in debye. Bonds and angles refer to the labels given in Fig. 1.

Molecule property	Acetate		3F-acetate	
	Theory	Expt.	Theory	Expt.
C–C	1.524	1.520	1.566	1.546
C–O _a	1.229	1.214	1.220	1.192
C–O _b	1.377	1.364	1.35	1.35
C–X ₁	1.12	1.10	1.371	1.325
C–X ₂	1.12	...	1.373	...
C–X ₃	1.12	...	1.356	...
OH	0.992	...	0.992	...
∠CCO _a	125.9	126.6	122.4	126.8
∠CCO _b	111.2	110.6	110.3	111.1
∠CCX ₁	111.4	...	114.0	109.5
∠CCX ₂	108.1	...	107.7	...
∠CCX ₃	109.3	...	109.6	...
Dipole	1.66	1.70	2.27	2.28

deviations from the experiment—the C–F bond lengths and some of the bond angles are only within about 4% of the experiment. Although this is likely to be better than the experimental error, to study this in more detail, we also considered the behavior of the molecules at a finite temperature. We performed constant temperature molecular-dynamics (MD) simulations at 300 K using a Nosé thermostat with a time step of 2 fs. Both molecules were run for 2.5 ps to equilibrate the system, followed by a run of 4.0 ps during which the data was collected. This demonstrated that the C–F bonds show much larger displacements at a finite temperature, with variations of up to 0.2 Å compared to 0.05 Å for the C–H bonds, which may play some role in the difference between the experimental and theoretical values for the C–F bond lengths. The mean bond lengths over the MD run (CH—1.12 Å, CF—1.37 Å) were the same for all C–X, showing that any asymmetry seen in Table I is a result of the zero-temperature, static approximation used. Finally, we note that the calculated net dipole for both molecules is in very good agreement with the experiments.

The (110) surface is characterized by bridging oxygen rows protruding from the surface and in-plane titaniums [see Fig. 1(b)]. Initial calculations for the surface itself¹⁴ were performed on a 36-atom cell [(1×1×3) in terms of the six-atom surface unit cell] using 12 *k*-points (4×4×1 *k*-point mesh), a mesh cutoff of 126 Ry, and an energy shift of 15

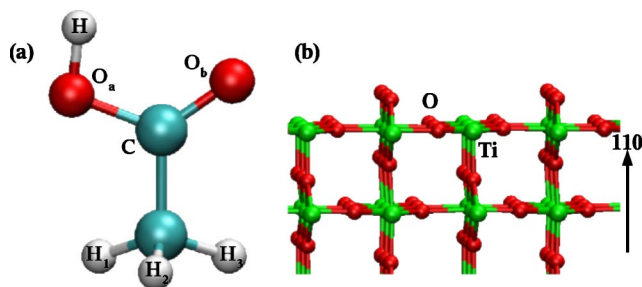


FIG. 1. Structure of (a) an isolated acetate molecule and (b) the TiO₂(110) surface.

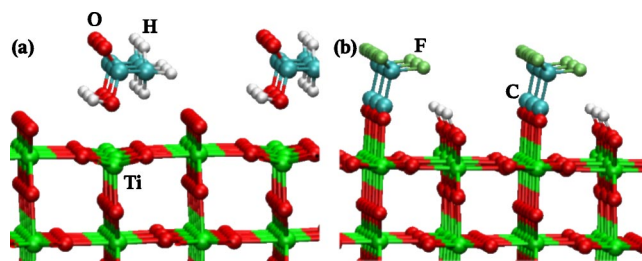


FIG. 2. Structure of a (a) molecularly adsorbed 0.5 ML coverage of acetate and a (b) dissociatively adsorbed 0.5 ML coverage of 3F-acetate.

meV. We found that this gives surface relaxations in reasonable agreement with the previous *ab initio* calculations¹¹ and experiments.⁶ To check the dependence of our results on the slab thickness, we also calculated the (1×1×6) and (1×1×7) slabs, and found that the surface relaxations have converged to less than 0.01 nm (and much better than this in most cases). This agrees with the previous studies of TiO₂ surface slab thickness.^{16,41}

IV. ADSORPTION

As stated previously, the simplest carboxylic acid, formate, has been shown both theoretically^{24,25} and experimentally^{21,22} to adsorb dissociatively on the (110) surface of TiO₂. At high coverages, the formate forms a *p*(2×1) structure corresponding to 0.5 ML (i.e., one molecule per two titaniums in the surface) with the two oxygens bonded to the surface titaniums and the proton bonding to the bridging oxygen sites. One would expect acetate to behave in a similar fashion, and experiments studying the orientation of acetate molecules on the surface^{26,27} indicate that it adsorbs with the C–C bond perpendicular to the surface, as for the formate. However, it is not immediately evident that the much less-acidic 3F-acetate should also adsorb dissociatively. Hence, for both acids, we have considered dissociative and molecular adsorption at different coverages (θ). The molecular adsorption results in either O_a (denoted molecular one, M1) or O_b (M2) [see Fig. 1(a)] bonding to an in-plane Ti, with the C–X₃ group oriented toward the bridging oxygen site. This geometry is shown in Fig. 2 for 0.5 ML of acetate M1, but the results for 3F-acetate are qualitatively similar, and the M2 can be considered as just a 180° rotation around the C–C bond.

In principle, dissociative adsorption can occur in several possible configurations. However, it has been shown previously for the formate²⁴ that saturating both carboxylate oxygens with bonds to the surface Ti ions is clearly favorable due to the symmetry of the bonding configuration. The proton bonds to the bridging oxygens, and the C–X₃ group is slightly tilted toward the OH species [see Fig. 2(b)]. Since the carboxylate group effectively occupies two Ti ions, we can consider only 0.5 ML coverage for this configuration.

The properties of the adsorbed layers are summarized in Table II. Here, we see that for both acetate and 3F-acetate, dissociative adsorption is overwhelmingly favored. The binding energy in both cases is about 2 eV, compared to less than 0.8 eV for the molecular configurations. This agrees with the experimental predictions on acetate,^{26,27} because

TABLE II. Comparison of adsorption properties for different coverages and adsorption mechanisms—coverage θ , binding energy E_B , and dipole perpendicular to the surface (the x and y dipole components are always zero). For the system D_L , we increased the surface size and number of adsorbed molecules by four. The mixed system consists of three 3F-acetate molecules and a single acetate molecule adsorbed in a mixed layer on the surface.

System	θ (ML)	E_B (eV)	Dipole (D)
Acetate M1	0.50	0.48	-0.90
Acetate M1	1.00	0.37	-1.60
Acetate M2	0.50	0.73	2.80
Acetate M2	1.00	0.32	4.30
Acetate D	0.50	1.92	2.15
Acetate D_L	0.50	7.81	8.60
3F-acetate M1	0.50	0.18	-1.32
3F-acetate M1	1.00	-2.00	-3.19
3F-acetate M2	0.50	0.32	2.33
3F-acetate M2	1.00	-2.31	3.10
3F-acetate D	0.50	1.92	-0.78
Mixed D	0.50	7.91	-0.37

this configuration is the only one that results in a C–C bond perpendicular to the surface. The interaction between molecular species is clearly stronger for 3F-acetate, so that at high coverage, the molecular configurations have a large negative binding energy. For acetate, the coverage effects are much smaller and E_B only drops by 0.1 eV in the M1 configuration and 0.4 eV in the M2, as the coverage is increased.

As a final check on the dissociative configuration and any symmetry effects, we increased the size of the acetate system by four, i.e., the coverage is the same, but we now have four molecules adsorbed on a larger TiO₂ slab. Table II shows that E_B and the dipole increase almost exactly by four, and we found no significant change in the adsorption geometry.

V. NC-AFM IMAGING

The most direct experimental study of the properties of these adsorbates on TiO₂ is the NC-AFM images mentioned previously.^{23,30–35} In the NC-AFM, the experiment is effectively measuring the force between the tip and the surface during scanning, so the brightest contrast in an image identifies the area of the strongest attractive tip-surface force. However, identifying the source of contrast remains difficult due to the unknown nature of the tip and the fact that the images are not necessarily a map of the physical topography of the surface.²⁹ This was clearly demonstrated in the NC-AFM images of a mixed monolayer of acetate and 3F-acetate.³⁰ The experiments assumed a dissociative adsorption for both acids, and further, because the molecules are of similar size, the adsorbed molecules would be equivalent in height. Hence, one might naively expect that the mixed layer would appear the same as the images of a uniform acetate layer.²³ This was not the case, as the images effectively contained two magnitudes of bright contrast spots, the brightest matching the dose of acetate and the less bright matching the dose of 3F-acetate. Previous studies of NC-AFM imaging²⁹ have demonstrated that, in the absence of strong covalent bonds between the tip and the surface, the force is strongly dependent on the interaction between the tip

and the surface electrostatic potential. Hence, Sasahara *et al.*³⁰ speculated that the difference in contrast over the molecules is due to the difference in the dipole moment of the two species.

In order to study this, we calculated a mixed monolayer on TiO₂ with three 3F-acetate molecules and one acetate molecule dissociatively adsorbed on the surface (the ratio of 3F-acetate to acetate in the experiments was roughly 3.6:1.0). The adsorption geometries do not change qualitatively from that of the uniform layers, and the two molecules are within 0.1 Å of each other in height. Table II shows that the binding energy of the mixed layer corresponds well with the binding energy of the three 3F-acetates and a single acetate molecule. The overall dipole of the mixed layer is -0.37 D (see Table II)—if we take three times the 3F-acetate dipole (3×-0.78 D) and add the acetate dipole (2.15 D), we get -0.19 D in fair agreement. Hence, it is reasonable to just take the dipoles from the uniform layers, and we see very clearly that acetate has a dipole three times larger (and in the opposite direction) to that of 3F-acetate. This indicates that the dipole moment, and hence, the electrostatic potential of the molecules is dominant in the imaging mechanism.

The difference in moment can be understood by comparing the Mulliken charges on atoms in the molecules. The C–X bond in acetate is actually more ionic ($C^{+0.47}-H^{-0.10}$) than in 3F-acetate ($C^{+0.15}-F^{-0.06}$), resulting in a larger moment. This agrees with the experimental difference in bond enthalpy with a more covalent C–F bond 2.2 eV stronger than a C–H bond.⁴⁰ Ostensibly, the dipoles for the isolated molecules (see Table I) seem to contradict this picture. However, considering only the moment in the direction along the molecule, which is perpendicular to the surface after adsorption (along C–C), we find 0.86 D for acetate and -1.67 D for 3F-acetate, and we see that the explanation is consistent.

VI. DISCUSSION

We have shown that both acetic acid and trifluoroacetic acid, similarly to formic acid, adsorb dissociatively on the TiO₂(110) surface. The carboxylate ion adsorbs with its two oxygens bonding to titanium ions in the surface, with the proton bonding to the bridging oxygen ions. The magnitude of difference between the binding energies for molecular and dissociative configurations is so large that we can be confident that it is beyond any inherent errors of the method. We also see that hydrogen bonding between O and OH for dissociative configurations and H and O for molecular configurations plays a role in the adsorption geometries—resulting in a tilting of the adsorbed molecules. One aspect absent from this study is the barriers for dissociation—although we see that dissociative adsorption is energetically favored in the static approximation, we cannot easily estimate the barrier. However, for acetate, experiments at room temperature observe a near perpendicular C–C bond, and our results show that this can only result from dissociative adsorption. Hence, it is likely that the barrier is small enough to be easily overcome at room temperature.

Our results seem to support the experimental interpretation³⁰ of the NC-AFM studies of acetate and 3F-acetate adsorption on the TiO₂(110) surface. The increased

dipole moment for acetate would result in an increased contrast compared to 3F-acetate, if the tip-surface interaction is dominated by electrostatics. However, although the dipole-dominated imaging mechanism appears consistent in theory and experiment, there are some issues that must be noted. If the tip formed strong covalent bonds with the molecules, then this would dominate the interaction, and any dipole effect would be secondary. It is likely that the C–X bonds are fairly inert, but this should be checked, especially with a reactive tip model. Furthermore, the experimental analysis³⁰ assumes that the tip apex was silicon. This would seem reasonable because the tip is fabricated from silicon and cleaned via sputtering periodically during scanning. However, one would expect the interaction between a dipole and a silicon tip to be very weak. Our calculations also show that for a silicon tip, the force is dominated by a repulsion between the electron orbitals, and the interaction is strongest over Ti rather than over the acid molecule. Fully interpreting the NC-AFM images is likely to require further studies considering the other tip models, which provide a tip-surface interaction dominated by electrostatics.

ACKNOWLEDGMENTS

This research has been supported by the Academy of Finland Center of Excellence Program (2000–2005) and the TEKES PINTA program. The authors are grateful to the Center of Scientific Computing, Espoo for computational resources, and the authors would also like to thank A. Y. Gal, Y. J. Lee, H. Onishi, and A. L. Shluger for the useful discussions. Atomic structure figures were produced with Visual Molecular Dynamics.⁴²

¹V. E. Henrich and P. A. Cox, *The Surface Science of Metal Oxides* (Cambridge University Press, Cambridge, 1996).

²A. L. Linsebigler, G. Lu, and J. T. Yates, *Chem. Rev.* (Washington, D.C.) **95**, 735 (1995).

³J. Lausmaa, *J. Electron Spectrosc. Relat. Phenom.* **81**, 343 (1996).

⁴U. Diebold, *Surf. Sci. Rep.* **48**, 53 (2003).

⁵U. Diebold, J. F. Anderson, K. O. Ng, and D. Vanderbilt, *Phys. Rev. Lett.* **77**, 1322 (1996).

⁶G. Charlton, P. B. Howes, C. L. Nicklin *et al.*, *Phys. Rev. Lett.* **78**, 495 (1997).

⁷D. Vogtenhuber, R. Podloucky, A. Neckel, S. G. Steinemann, and A. J. Freeman, *Phys. Rev. B* **49**, 2099 (1994).

⁸M. Ramamoorthy, R. D. King-Smith, and D. Vanderbilt, *Phys. Rev. B* **49**, 7709 (1994).

⁹M. Ramamoorthy, D. Vanderbilt, and R. D. King-Smith, *Phys. Rev. B* **49**, 16721 (1994).

¹⁰P. J. D. Lindan, N. M. Harrison, and M. J. Gillan, *Phys. Rev. Lett.* **80**, 762 (1998).

¹¹N. M. Harrison, X. G. Wang, J. Muscat, and M. Scheffler, *Faraday Discuss.* **114**, 305 (1999).

¹²A. T. Paxton and L. Thiên-Nga, *Phys. Rev. B* **57**, 1579 (1998).

¹³R. Schaub, E. Wahlström, A. Rønna, E. Lægsgaard, E. Stensgaard, and F. Besenbacher, *Science* **299**, 377 (2003).

¹⁴A. S. Foster, O. H. Pakarinen, J. M. Airaksinen, J. D. Gale, and R. M. Nieminen, *Phys. Rev. B* **68**, 195410 (2003).

¹⁵S. P. Bates, G. Kresse, and M. J. Gillan, *Surf. Sci.* **409**, 336 (1998).

¹⁶J. Muscat, N. M. Harrison, and G. Thornton, *Phys. Rev. B* **59**, 2320 (1999).

¹⁷I. M. Brookes, C. A. Muryn, and G. Thornton, *Phys. Rev. Lett.* **87**, 266103 (2001).

¹⁸G. Liu, J. A. Rodriguez, Z. Chang, J. Hrbek, and L. González, *J. Phys. Chem. B* **106**, 9883 (2002).

¹⁹E. Wahlström, N. Lopez, R. Schaub *et al.*, *Phys. Rev. Lett.* **90**, 026101 (2003).

²⁰M. D. Rasmussen, L. M. Molina, and B. Hammer, *J. Chem. Phys.* **120**, 988 (2004).

²¹H. Onishi and Y. Iwasawa, *Chem. Phys. Lett.* **226**, 111 (1994).

²²S. A. Chambers, S. Thevuthasan, Y. J. Kim, G. S. Hermann, Z. Wang, E. Tober, R. Ynzunza, and J. Morais, *Chem. Phys. Lett.* **267**, 51 (1997).

²³K. I. Fukui, H. Onishi, and Y. Iwasawa, *Chem. Phys. Lett.* **280**, 296 (1997).

²⁴S. P. Bates, G. Kresse, and M. J. Gillan, *Surf. Sci.* **409**, 336 (1998).

²⁵P. Käckell and K. Terakura, *Surf. Sci.* **461**, 191 (2000).

²⁶Q. Guo, I. Cocks, and E. M. Williams, *J. Chem. Phys.* **106**, 2924 (1997).

²⁷A. Gutiérrez-Sosa, P. Martínez-Escolano, H. Raza, R. Lindsay, P. L. Wincott, and G. Thornton, *Surf. Sci.* **471**, 163 (2001).

²⁸*Noncontact Atomic Force Microscopy*, edited by S. Morita, R. Wiesendanger, and E. Meyer (Springer, Berlin, 2002).

²⁹W. Hofer, A. S. Foster, and A. L. Shluger, *Rev. Mod. Phys.* **75**, 1287 (2003).

³⁰A. Sasahara, H. Uetsuka, and H. Onishi, *Phys. Rev. B* **64**, 121406 (2001).

³¹A. Sasahara, H. Uetsuka, and H. Onishi, *Surf. Sci. Lett.* **481**, L437 (2001).

³²A. Sasahara, H. Uetsuka, and H. Onishi, *J. Phys. Chem. B* **105**, 1 (2001).

³³H. Onishi, A. Sasahara, H. Uetsuka, and T. Ishibashi, *Appl. Surf. Sci.* **188**, 257 (2002).

³⁴A. Sasahara, H. Uetsuka, T. Ishibashi, and H. Onishi, *Appl. Surf. Sci.* **188**, 265 (2002).

³⁵A. Sasahara, H. Uetsuka, and H. Onishi, *Langmuir* **19**, 7474 (2003).

³⁶J. Junquera, O. Paz, D. Sánchez-Portal, and E. Artacho, *Phys. Rev. B* **64**, 235111 (2001).

³⁷J. M. Soler, E. Artacho, J. D. Gale, A. García, J. Junquera, P. Ordejón, and D. Sánchez-Portal, *J. Phys.: Condens. Matter* **14**, 2745 (2002).

³⁸J. P. Perdew, K. Burke, and M. Ernzerhof, *Phys. Rev. Lett.* **77**, 3865 (1996).

³⁹S. G. Louie, S. Froyen, and M. L. Cohen, *Phys. Rev. B* **26**, 1738 (1982).

⁴⁰*Handbook of Chemistry and Physics*, 84th ed., edited by D. R. Lide (CRC, Boca Raton, 2003).

⁴¹S. H. Ke, T. Uda, and K. Terakura, *Phys. Rev. B* **65**, 125417 (2002).

⁴²W. Humphrey, A. Dalke, and K. Schulten, *J. Mol. Graphics* **14**, 33 (1996).